Materials Science

http://www.aimspress.com/journal/Materials/

AIMS Materials Science, 3(4): 1507-1519.
DOI: 10.3934/matersci.2016.4.1507.
Received: 25 August 2016
Accepted: 31 October 2016
Published: 10 November 2016

*Research article*

# A Mode-III strip saturation model for two collinear semi-permeable cracks in a piezoelectric media

**R.R.Bhargava[1], Kamlesh Jangid[2,*], and Pavitra Tripathi[1]**

[1] Department of Mathematics, Indian Institute of Technology, Roorkee-247667, India
[2] Department of Humanities English & Applied Sciences, Rajasthan Technical University, Kota-324010, India

[*] **Correspondence:** Email: jangidkamlesh7@gmail.com; Tel: +91-9694434826.

**Abstract:** In this paper, a mode-III strip-saturation model is proposed for a piezoelectric ceramic plate weakened by two equal collinear, semi-permeable hairline cracks. A mathematical model is obtained using Stroh's formalism and solved using matrix Hilbert problem. Analytic closed form expressions are derived for various fracture parameters such as crack sliding displacement, crack opening potential drop, field intensity factor and energy release rate. An illustrative numerical case study is presented for impermeable, semi-permeable and permeable crack face boundary conditions for different piezo-ceramics. The results obtained are presented graphically, discussed and concluded. It is observed that the model proposed is capable of crack arrest under small-scale electric saturation.

**Keywords:** crack sliding displacement; energy release rate; piezoelectric ceramics; saturation zone; semi-permeable cracks

## 1. Introduction

Due to intrinsic electro-mechanical coupling effect, piezoelectric materials have vast utility in many engineering devices, such as sensors, transducers, actuator components. But, under the action of electromechanical loadings, these piezoelectric materials could fail prematurely due to defects, e.g., cracks, holes, etc., arising during their manufacturing process over loads/fatigue/aging etc. This has made it important subject for study of their cracking/failure mechanics. Lots of research has been carried on a crack weakening a piezo-ceramic sensor etc., from 1990. Due to the tendency of developing multiple cracks in piezoelectric ceramics, the interaction amongst these cracks and their effects on the ceramic play an important role in fracture behavior of these ceramics and this makes the subject matter of the investigations of this paper.

The concept of strip-saturation model [1] was introduced by Gao for a cracked poled piezoelectric

plate, based on the concept of Dugdale model for strip-yield model [2] for metals. The extended case of strip-saturation model for a semi-permeable and for a conductive crack face boundary conditions [3, 4] was solved. Wang [5] gave a fully anisotropic analysis proposed by Gao et al. [1]. Li [6] re-examined the strip-saturation model for a permeable cracked piezoelectric ceramic to analyze fracture toughness of piezoelectric ceramic. Jeong et al. [7] proposed a strip-saturation model for cracked ferroelectric ceramic with perfect saturation under electrical loading.

Using complex function theory Beom et al. [8] analysed a strip-saturation model for an electrostrictive material under pure electric loading. Fan et al. [9] analysed a polarization saturation model for a non-linear semi-permeable crack in piezoelectric plane.

Bhargava and Jangid [10] were the first one to propose a strip-saturation model for two collinear cracks in a poled piezo-ceramic under mode-I conditions. They further extended [11] the strip-saturation when saturation zone developed at adjacent interior tips of the cracks get coalesced.

Zhang and Lee [12] investigated the problem of two collinear electrically dielectric cracks in a piezoelectric layer, within the frame work of linear piezoelectricity. Bui et al. [13, 14, 15] investigated the crack problems using BEM, DDM and XFEM methods for various crack face boundary conditions.

As we know, an analytic solution of the problem in closed form has some advantage over numerical and approximate solutions, which can serve a benchmark for the purpose of judging the accuracy and efficiency of various numerical and approximate methods.

Therefore, present paper deals with the problem of strip-saturation model for two collinear semi-permeable hairline cracks weakening a poled piezoelectric ceramic under mode-III conditions. Stroh formalism and complex variables employed to obtain the solution. Closed from analytic expressions are derived for various fracture parameters. A case study is presented for cracked piezo-ceramics $PZT-5H$, $PZT-6B$, $PZT-7A$ under permeable, semi-permeable and impermeable crack face boundary conditions. Results obtained are presented graphically, discussed and concluded. It is seen that the model proposed is capable of crack arrest.

## 2. Fundamental Formulation and Solution Methodology

As are well known for out of plane problem, displacement components $u_i(i = x, y, z)$ are defined as

$$u_x(x, y, z) = 0, u_y(x, y, z) = 0, \text{and } u_z(x, y, z) = w(x, y)$$

and for in-plane electric field problem, the electric field component $E_i(x, y, z)$ may be defined as

$$E_x(x, y, z) = E_x(x, y) = -\phi_{,x}\,, E_y(x, y, z) = E_y(x, y) = -\phi_{,y} \text{ and } E_z(x, y, z) = 0$$

where "$\phi$" denotes the electric potential and comma after the function denotes the partial differentiation with respect to argument following it.

Gradient equations may be written as,

$$\epsilon_{zi} = w_{,i} \text{ and } E_i = -\phi_{,i} \text{ where } i = x, y. \tag{1}$$

Constitutive equations for stress components, $\sigma_{zi}$ and electric displacement components, $D_i, (i = x, y)$ may be written as

$$\sigma_{zi} = c_{44}w_{,i} + e_{15}\phi_{,i}, \quad D_i = e_{15}w_{,i} - k_{11}\phi_{,i} \tag{2}$$

where $c_{44}$, $e_{15}$ and $k_{11}$ are elastic, piezoelectric and dielectric constant, respectively.

Equilibrium equations for stresses in absence of body force and for electric displacement in absence of body charge may be written as

$$\sigma_{ij,j} = 0,\ D_{i,i} = 0. \tag{3}$$

The general solution of Eq. (2) may be expressed in terms of generalized stress function $\Phi$ and generalized displacement vector $\mathbf{u} = [w, \phi]^T$, where superscript $T$ denotes the transpose of the matrix.

$$\mathbf{u}_{,1} = AF(z) + \overline{AF(z)} \tag{4}$$

$$\Phi_{,1} = BF(z) + \overline{BF(z)} \tag{5}$$

where $z = (x + iy = x_1 + ix_2)$, $F(z) = \frac{df(z)}{dz}$, $f(z)$ being an analytic function and $A$, $B$ stand for material constant matrix defined as,

$$A = I,\ B = iB_0 = i\begin{pmatrix} c_{44} & e_{15} \\ e_{15} & -k_{11} \end{pmatrix}.$$

## 3. Statement and Solution of the Problem

Let a piezoelectric material occupy the region $oxy$ and is poled along $oy$ direction. The plate is cut along $ox$ direction forming two equal finite hairline straight cracks $L_1$ and $L_2$. These occupy the region $y = 0$, $[-d, -c]$ and $[d, c]$ respectively. Out-of-plane stress, $\sigma_{zy} = \tau_0$, is applied at remote boundary as $x_2 \to \infty$ and also in-plane electric displacement, $D_2{}^{\infty}$ applied along $oy$ direction. Due to prescribed forces, the cracks open in self-similar fashion forming a small saturation zone in a strip ahead each tip of the cracks. To arrest the cracks from further opening, the developed zones are subjected to normal cohesive saturation limit electrical displacement $D_2 = D_s$. The schematic configuration of the problem is depicted in Figure 1.

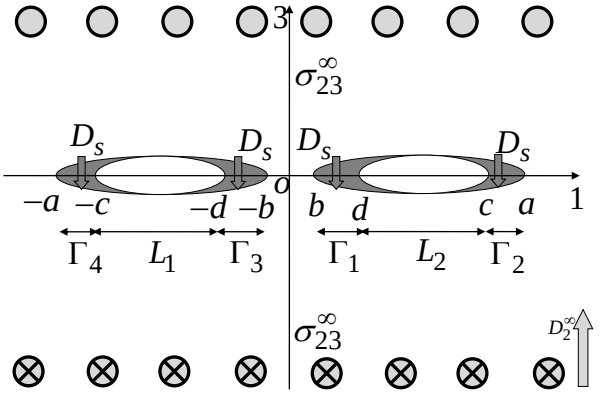


**Figure 1. Schematic representation of the problem.**

Mathematically boundary conditions of the problem may be written as,
(i) $\sigma_{zi}{}^{+} = \sigma_{zi}{}^{-} = 0,\ D_2 = D_r,\quad$ for $d \le |x| \le c$,
(ii) $\sigma_{zy} = \tau_0,\ D_2 = D_2{}^{\infty},\quad$ for $|y| \to \infty$,
(iii) $\sigma_{zi}{}^{+} = \sigma_{zi}{}^{-},\ D_2{}^{+} = D_2{}^{-} = D_s,\quad$ for $b \le |x| \le d\quad$ and $c \le |x| \le a$,
(iv) $\Phi_{,1}(x)^{+} = \Phi_{,1}(x)^{-} = -V,\quad$ for $d \le |x| \le c$,

where, $V = [0, 0, \tau_0, {D_2}^{\infty}]^T$ and $D_r$ denotes electric crack condition parameter which is of value 1 for permeable case, zero for impermeable case and lies between (0, 1) for semi-permeable case.

From the condition of continuity of $\Phi_{,1}$ on the $ox$-axis barring the interval $d \leq |x| \leq c$ yields vector Hilbert problem.

$$[BF(x) - \overline{BF(x)}]^{+} - [BF(x) - \overline{BF(x)}]^{-} = 0.$$

Solution of which may be written as,

$$BF(z) = \overline{BF(z)} = h(z)(\text{say}) \tag{6}$$

The boundary condition $(iv)$ together with Eqs. (5), (6) yields

$$h^{+}(x) + h^{-}(x) = -V, \quad \text{for} \quad d \leq |x| \leq c \tag{7}$$

Introducing new complex function vector as,

$$\Omega(z) = [\Omega_1(z), \Omega_2(z), \Omega_3(z), \Omega_4(z)]^T$$

and

$$h(z) = [H^R]^{-1}\Omega(z) = \Lambda\Omega(z)$$

where

$$H^R = 2Re[iAB^{-1}] \quad \text{and } \Lambda = \begin{pmatrix} \Lambda_{33} & \Lambda_{34} \\ \Lambda_{43} & \Lambda_{44} \end{pmatrix} = [H^R]^{-1}.$$

Consequently Eq. (7) can be written as,

$$\Lambda[\Omega^{+}(x) + \Omega^{-}(x)] = -V \quad \text{for} \quad d < |x| < c. \tag{8}$$

Above equation in component form leads to the scalar Hilbert problem

$$\Lambda_{33}[{\Omega_3}^{+}(x) + {\Omega_3}^{-}(x)] + \Lambda_{34}[{\Omega_4}^{+}(x) + {\Omega_4}^{-}(x)] = -\tau_0, \tag{9}$$

$$\Lambda_{43}[{\Omega_3}^{+}(x) + {\Omega_3}^{-}(x)] + \Lambda_{44}[{\Omega_4}^{+}(x) + {\Omega_4}^{-}(x)] = D_r - {D_2}^{\infty}. \tag{10}$$

Solving these equations for $\Omega_3(z)$ and $\Omega_4(z)$ together with boundary conditions $(ii), (iii)$ and single-valuedness of displacement from Muskhelishvili [16], we obtain

$$\Omega_3(z) = \frac{1}{2\triangle}\left[\tau_0\Lambda_{44} + (D_r - D_2^{\infty})\right]\left\{\frac{z^2 - c^2\lambda^2}{\sqrt{(z^2 - d^2)(z^2 - c^2)}} - 1\right\}, \tag{11}$$

where, $\triangle = \Lambda_{33}\Lambda_{44} - \Lambda_{34}\Lambda_{43}$, $\lambda^2 = \frac{E(k)}{F(k)}$ and $k = \frac{(c^2 - d^2)}{c^2}$, $E(k)$and $F(k)$ denote complete elliptic integral of first and second kind, respectively.

The general solution of Eq. (10) yields $\Omega_4(z)$, once $\Omega_3(z)$ is obtained.

$$\Omega_4(z) = -\frac{\Lambda_{43}}{\Lambda_{44}}\Omega_3(z) + \frac{D_r - {D_2}^{\infty}}{2\Lambda_{44}} + \frac{1}{\Lambda_{44}}\left[\frac{P_2(z)}{2X_1(z)} + \frac{D_s - D_r}{2\pi i X_1(z)}\int \frac{X_1(t)}{t - z}dt\right] \tag{12}$$

where $X_1(z) = \sqrt{(z^2 - a^2)(z^2 - b^2)}$, $P_2(z) = G_0z^2 + G_1z + G_2$ and $\Gamma = \bigcup_{i=1}^{4}\Gamma_i$.

Here, $\Gamma_i$ being the saturation zones occupying the interval $b \le |x| \le d$ and $c \le |x| \le a$ on $ox$-axis. Arbitrary constant, $G_0$, determined using boundary condition at infinity; $G_1$ and $G_2$ are determined using single-valuedness condition of displacement around cracks. After a lengthy calculation, one finally obtain $\Omega_4(z)$ as,

$$\Omega_4(z) = -\frac{\Lambda_{43}}{\Lambda_{44}}\Omega_3(z) + \frac{(D_2{}^{\infty} - D_r)}{2\Lambda_{44}}\left\{\frac{z^2 - a^2{\lambda_1}^2}{X_1(z)} - 1\right\} - \frac{(D_s - D_r)}{\pi\Lambda_{44}X_1(z)}\Big[(z^2 - a^2{\lambda_1}^2)(\frac{\pi}{2} - \psi_1 + \psi_2)$$
$$-(a^2 - b^2)(\sin\psi_1\cos\psi_1 - \sin\psi_2\cos\psi_2) + ad\{E(\psi_1, k_1) - {\lambda_1}^2F(\psi_1, k_1)\}$$
$$-ac\{E(\psi_2, k_1) - {\lambda_1}^2F(\psi_2, k_1)\} - X_1(z)(\frac{\pi}{2} - \theta_1 + \theta_2)\Big] \quad (13)$$

where

$${\lambda_1}^2 = \frac{E(k_1)}{K(k_1)}, \quad k_1 = \frac{(a^2 - b^2)}{a^2}, \quad \sin^2\psi = \frac{(a^2 - {x_1}^2)}{(a^2 - b^2)}, \quad \tan^2\theta = \frac{(b^2 - z^2)}{a^2 - z^2}\tan^2\psi$$
$$\sin^2\psi_1 = \frac{(a^2 - d^2)}{(a^2 - b^2)}, \quad \sin^2\psi_2 = \frac{(a^2 - c^2)}{(a^2 - b^2)}$$

## 4. Applications

In this section, we present various applications of the problem for finding crack sliding displacement, crack opening potential drop, intensity factors, saturation zone lengths and energy release rate.

### *4.1. Crack Sliding Displacement (CSD)*

The jump displacement vector $\Delta\mathbf{u}$ is defined as

$$i\Delta\mathbf{u}_{,1} = \mathbf{H}^R[\mathbf{B}\mathbf{F}^+(x) - \mathbf{B}\mathbf{F}^-(x)] = \Omega^+(x) - \Omega^-(x) \quad (14)$$

Crack sliding displacement is the relative crack face opening between the two surfaces of the crack. Crack sliding displacement can be used as a measure of the toughness of the materials under mode-III deformation. CSD, $\Delta w$, is determined substituting, $\Omega_3(z)$, from Eq. (11) into Eq. (14) and noting $\Delta w = 0$ at $x = \pm d, \pm c$, one obtains

$$\Delta w_{,1} = -i\{\Omega_3^+(x) - \Omega_3^-(x)\}.$$

On integrating

$$\Delta w = c\left\{\frac{\tau_0\Lambda_{44} + (D_r - D_2{}^{\infty})\Lambda_{34}}{\Lambda_{33}\Lambda_{44} - \Lambda_{34}\Lambda_{43}}\right\}\Big(E(\chi, k) - \lambda^2F(\chi, k)\Big) \quad (15)$$

where, $\sin^2\chi = \dfrac{c^2 - x_1^2}{c^2 - d^2}$.

### *4.2. Crack Potential Drop (COP)*

Crack opening potential drop is the electric potential difference between the two surfaces of the crack. Same as CSD, COP is used to measure the fracture and fatigue of materials. COP, $\Delta\phi$, can be obtained using,

$$\Delta u_{4,1} = -i\{{\Omega_4}^+(x) - {\Omega_4}^-(x)\}$$

Integrating above equation, substituting $\Omega_4(z)$ from Eq. (13) into Eq. (14), then taking limit $x \to c$ and $x \to d$, we obtain

$$\Delta\phi(d) = -\frac{D_s - D_r}{\pi\Lambda_{44}}\left\{R_3 - \pi a\frac{D_2^{\infty} - D_r}{D_s - D_r}R_4\right\}, \tag{16}$$

$$\Delta\phi(c) = \frac{D_s - D_r}{\pi\Lambda_{44}}\left\{R_5 - \pi a\frac{D_2^{\infty} - D_r}{D_s - D_r}\left(E(\psi_2, k_1) - \lambda_1^2 F(\psi_2, k_1)\right)\right\}, \tag{17}$$

where, $R_3$, $R_4$ and $R_5$ can be found from appendix A.

### *4.3. Saturation Zone Length*

Saturation zone length is obtained using Dugdale [2] hypothesis to be true for electric displacement to remain finite at every point of the body, consequently at the tips $x = a$ and $x = b$ yields following two non-linear transcendental equations.

$$\left(\frac{b^2}{a^2} - {\lambda_1}^2\right)\left(\frac{\pi}{2}\frac{{D_2}^{\infty} - D_r}{D_s - D_r} - \frac{\pi}{2} + \psi_1 - \psi_2\right) + {k_1}^2(\sin\psi_1\cos\psi_1 - \sin\psi_2\cos\psi_2)$$
$$-\frac{d}{a}\{E(\psi_1, k_1) - {\lambda_1}^2 F(\psi_1, k_1)\} + \frac{c}{a}\{E(\psi_2, k_1) - {\lambda_1}^2 F(\psi_2, k_1)\} = 0, \tag{18}$$

and

$$(1 - {\lambda_1}^2)\left(\frac{\pi}{2}\frac{{D_2}^{\infty} - D_r}{D_s - D_r} - \frac{\pi}{2} + \psi_1 - \psi_2\right) + {k_1}^2(\sin\psi_1\cos\psi_1 - \sin\psi_1 - \sin\psi_2\cos\psi_2)$$
$$-\frac{d}{a}\{E(\psi_1, k_1) - {\lambda_1}^2 F(\psi_1, k_1)\} + \frac{c}{a}\{E(\psi_2, k_1) - {\lambda_1}^2 F(\psi_2, k_1)\} = 0. \tag{19}$$

From these, $a$ and $b$ are determined and saturation zone lengths are then determined from $(a - c)$ and $(b - d)$.

### *4.4. Field Intensity Factors*

In Piezoelectric materials, near the tip of the crack, each stress component is proportional to a constant $K$. And if this constant is known then the state of stress at the tip of crack can be determined. This constant is known as stress intensity factor. Stress and electric displacement intensity factors at the tip $x = c$ and $d$ are determined in this section.

#### 4.4.1. Stress Intensity Factor (SIF)

Mode-III stress intensity factor ${K_d}^{\tau}$ at the tip $x = d$ can be determined by this formula,

$$\begin{aligned} {K_d}^{\tau} &= \lim_{x \to d^-} \sqrt{2\pi(d - x)}\sigma_{zy}(x, 0) \\ &= -\{\tau_0 + (D_r - {D_2}^{\infty})\frac{\Lambda_{34}}{\Lambda_{44}}\}\sqrt{\frac{\pi}{d(d^2 - c^2)}}(d^2 - c^2\lambda^2). \end{aligned} \tag{20}$$

Similarly, SIF at tip $x = c$ is obtained as,

$$\begin{aligned} {K_c}^{\tau} &= \lim_{x \to c^+} \sqrt{2\pi(x - c)}\sigma_{zy}(x, 0) \\ &= \{\tau_0 + (D_r - {D_2}^{\infty})\frac{\Lambda_{34}}{\Lambda_{44}}\}\sqrt{\frac{\pi}{c(c^2 - d^2)}}(c^2 - c^2\lambda^2). \end{aligned} \tag{21}$$

4.4.2. Electric Displacement Intensity Factor (EDIF)

Mode-III, EDIF obtained at the tip $x = b$ from

$$\begin{aligned} K_b^D &= \lim_{x\to b^-} \sqrt{2\pi(b-x)}D_y(x,0) \\ &= \sqrt{\frac{\pi}{b(a^2-b^2)}}[({D_2}^\infty - D_r)(b^2 - a^2{\lambda_1}^2) - \frac{2}{\pi}(D_s - D_r)\{(b^2 - a^2{\lambda_1}^2)(\frac{\pi}{2} - \psi_1 + \psi_2) \\ &\quad - (a^2 - b^2)(\sin\psi_1\cos\psi_1 - \sin\psi_2\cos\psi_2) + da\left(E(\psi_1,k_1) - {\lambda_1}^2F(\psi_1,k_1)\right) \\ &\quad - ca\left(E(\psi_2,k_1) - {\lambda_1}^2F(\psi_2,k_1)\right)\}] \end{aligned} \tag{22}$$

Analogously EDIF at the tip $x = a$ is obtained as

$$\begin{aligned} K_a^D &= \lim_{x\to a^+} \sqrt{2\pi(x-a)}D_y(x,0) \\ &= -\sqrt{\frac{\pi}{a(a^2-b^2)}}[({D_2}^\infty - D_r)(a^2 - a^2\lambda^2) - \frac{2(D_s - D_r)}{\pi}\{(a^2 - a^2{\lambda_1}^2)(\frac{\pi}{2} - \psi_1 + \psi_2) \\ &\quad - (a^2 - b^2)(\sin\psi_1\cos\psi_1 - \sin\psi_2\cos\psi_2)\} + da\left(E(\psi_1,k_1) - {\lambda_1}^2F(\psi_1,k_1)\right) \\ &\quad - ca\left(E(\psi_2,k_1) - {\lambda_1}^2F(\psi_2,k_1)\right)\}]. \end{aligned} \tag{23}$$

While mode-III strain intensity factors ${K_d}^\epsilon$ and ${K_c}^\epsilon$ and mode-III electric field intensity factors, ${K_b}^E$ and ${K_a}^E$ factors are calculated from

$$K_d^\epsilon = \frac{e_{15}K_b^D + k_{11}K_d^\tau}{e_{15}^2 + k_{11}c_{44}}, \tag{24}$$

$$K_c^\epsilon = \frac{e_{15}K_a^D + k_{11}K_c^\tau}{e_{15}^2 + k_{11}c_{44}}, \tag{25}$$

$$K_b^E = \frac{c_{44}K_b^D - e_{15}K_d^\tau}{e_{15}^2 + k_{11}c_{44}}, \tag{26}$$

$$K_a^E = \frac{c_{44}K_a^D - e_{15}K_c^\tau}{e_{15}^2 + k_{11}c_{44}}. \tag{27}$$

*4.5. Energy Release Rate (ERR)*

ERR $G_d$ and $G_c$ at the tips $x = d$ and $x = c$, respectively computed using,

$$G_d = \frac{1}{2}[{K_d}^\tau {K_d}^\epsilon - {K_b}^D {K_b}^E], \tag{28}$$

$$G_c = \frac{1}{2}[{K_c}^\tau {K_c}^\epsilon - {K_a}^D {K_c}^E]. \tag{29}$$

## 5. A Special Case

In order to verify the above derived results, let us consider a strip electric saturation model of single crack problem in piezoelectric material. The crack occupy the interval $(-c, c)$ and developed saturation zone occupy the interval $c < |x| < a$; with semi-permeable electric boundary condition, then the above Eqs. (11) and (13) with $b = d = 0$, reduces to the results of Wang [5].

## 6. Case Study

A numerical case study is presented for various crack face boundary conditions for ceramics $PZT-5H$, $PZT-6B$ and $PZT-7A$. The crack lengths are taken to be $10mm$ each and $D_s = 0.03C/m^2$.

The material parameter for piezo-ceramics given in Table 1 below taken from, Ou and Wu [17].

**Table 1. Material constants.**

| Material/ Constants | $c_{44}(10^{10}Nm^{-2})$ | $e_{15}(Cm^{-2})$ | $k_{11}(10^{-10}C/Vm)$ |
|---|---|---|---|
| PZT-5H | 2.30 | 17.44 | 150.3 |
| PZT-6B | 2.71 | 4.60 | 36.0 |
| PZT-7A | 2.54 | 9.70 | 81.1 |

### *6.1. Variation of Crack Sliding Displacement (CSD) over Crack Rims*

Figure 2 depicts the variation of CSD over the crack rims. It is observed that CSD is symmetrical and parabolically varying with respect to middle point and is maximum at the center point of crack and then reduces till it becomes zero at end points. Also CSD is maximum for impermeable boundary condition and almost three times less for semi-permeable case as compared to that for impermeable case. CSD further reduces for permeable crack face boundary conditions and crack opens least for this case.

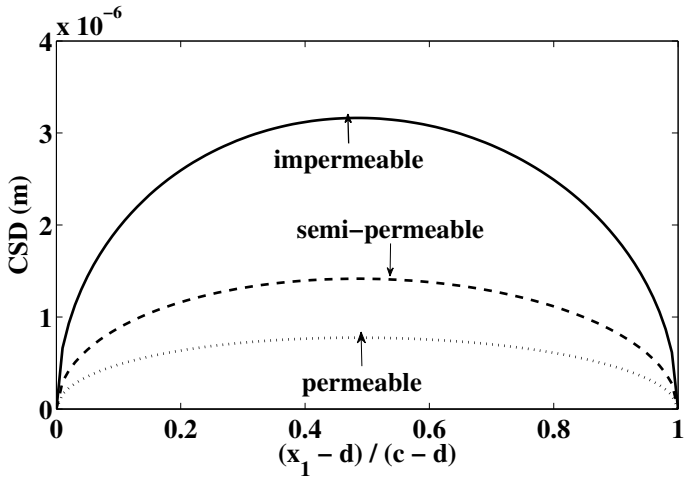


**Figure 2. CSD over the crack surface.**

### *6.2. Variation of CSD for Different Piezoceramics*

The opening of crack on different piezoceramics is depicted in Figure 3. It is noted that crack opens least for $PZT-5H$ ceramic and maximum for $PZT-6B$ ceramic. It may assists the designers for the correct selection of the ceramic for desired purposes.

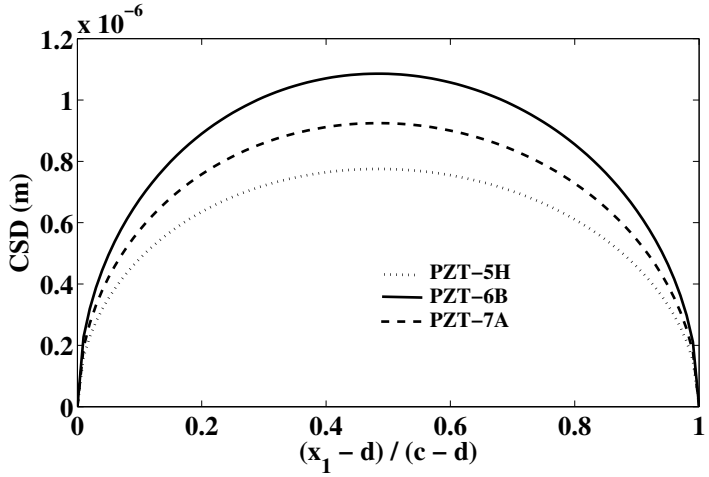


**Figure 3. CSD for different piezoceramics.**

### *6.3. Effect of Electric Load on Electric Displacement Intensity Factor*

Variation of electric displacement intensity factor $K^D$ versus prescribed electric displacement ${D_2}^{\infty}$, for impermeable, semi-permeable and permeable crack face conditions is plotted in Figure 4 at interior and exterior tips of the crack. It is observed that $K^D$ decreases almost linearly as ${D_2}^{\infty}$ is increased for all the cases. It is noted that $K^D$ is higher at inner tip for all three crack face boundary conditions. Also $K^D$ is maximum for impermeable case followed by semi-permeable case, and is minimum for permeable case. Same trend is followed at the interior tip of the crack.

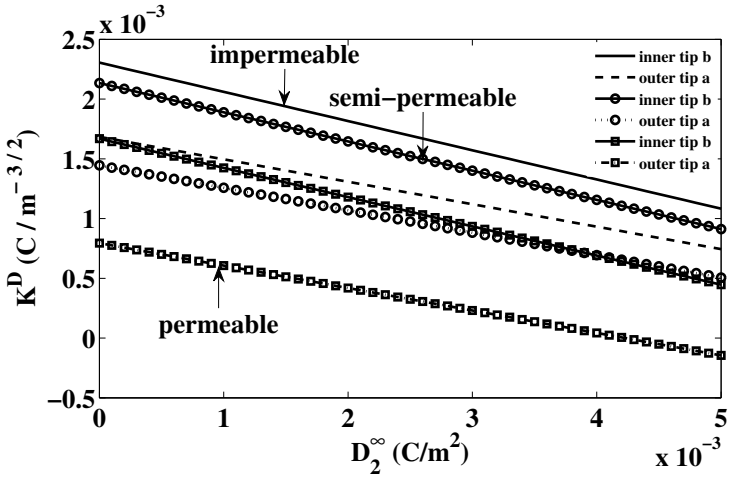


**Figure 4. Variation of $K^D$ with respect to ${D_2}^{\infty}$.**

### *6.4. Effect of Electric Displacement on Energy Release Rate*

Energy release rate versus ${D_2}^{\infty}$ variation is presented in Figure 5. ERR decreases continuously with increasing ${D_2}^{\infty}$. The decrease for impermeable boundary condition is more sharp as compared to that for semi-permeable and permeable case. At the outer tip $d$, the variation for semi-permeable and permeable cases, decrease in ERR is very close to each other while for impermeable case, variation is more steep and away from semi-permeable and permeable case.

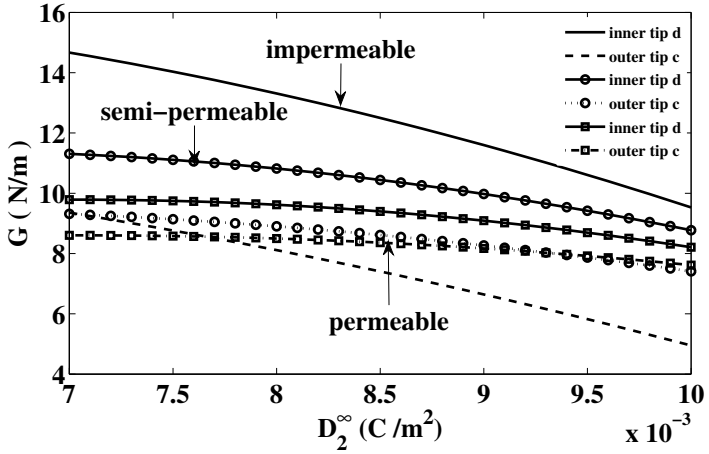


**Figure 5. Variation of energy release rate versus $D_2{}^{\infty}$.**

### *6.5. Stress Intensity Variation at the Crack Tip*

Figure 6 presents the variation of SIF, $K^{\tau}$ at the inner tip $x_1 = d$ and outer tip $x_1 = c$ of the crack with respect to the inter-crack distance. It is observed that stress concentration is maximum for the case of impermeable crack face boundary condition followed by semi-permeable crack face boundary condition and least for permeable crack face boundary condition, as expected. For all the three cases the SIF variation at inner crack tip show a slight parabolic decrease for smaller values of inter crack distance to crack length ratio and then stabilizes to a uniform constant variation for $d/a > 1.5$. The same is true for the variation at the outer tip but in this case, the variation is more flat as compared to that in the case of inner tip.

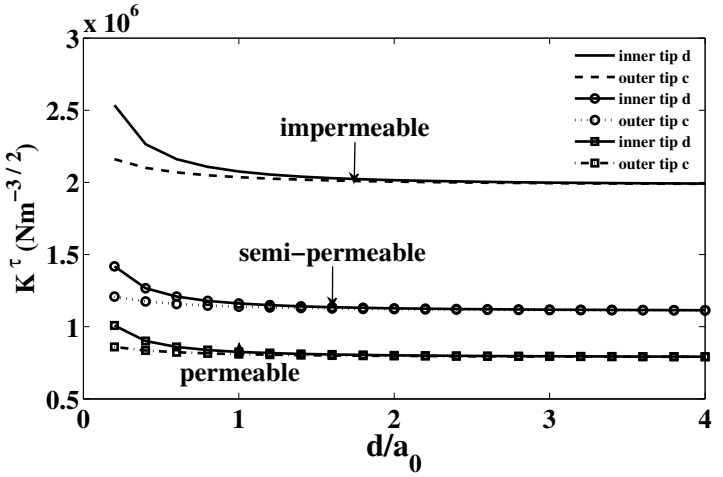


**Figure 6. Variation of $K^{\tau}$ with respect to inter-crack distance.**

## 7. Conclusions

- The proposed strip-saturation model is capable of crack arrest for small electric yielding case. The reduction in energy release rate confirms it.

- The study of CSD on different piezoceramic presented may assists the designers for the correct choice of the piezoceramic required for specific purpose.
- There is more stress concentration around crack tip for impermeable crack face boundary condition as compared to that for semi-permeable and permeable case and is least for permeable case.

## Acknowledgments

Authors are grateful to **Prof R. D. Bhargava** {Senior Professor(retd.), Indian Institute of Technology Bombay, Mumbai, India} for continuous encouragement during course of this work. The second author wishes to gratefully acknowledge the support of RTU, Kota, India.

## Conflict of Interest

All authors declare no conflict of interest in this paper.

## A. Appendix

$$R_1 = \frac{d}{a}\left(E(\psi_1,k_1) - \lambda_1^2 F(\psi_1,k_1)\right) - \frac{c}{a}\left(E(\psi_2,k_1) - \lambda_1^2 F(\psi_2,k_1)\right) - k_1^2\left(\sin\psi_1\cos\psi_1 - \sin\psi_2\cos\psi_2\right), \tag{A.1}$$

$$R_2 = a\lambda_1^2\left(\frac{\pi}{2} - \psi_1 + \psi_2\right) - aR_1, \tag{A.2}$$

$$G(d,c) = -d\ln\left(\frac{\sqrt{(d^2-b^2)(a^2-c^2)} + \sqrt{(a^2-d^2)(c^2-b^2)}}{\sqrt{(d^2-b^2)(a^2-c^2)} - \sqrt{(a^2-d^2)(c^2-b^2)}}\right) + \frac{2b^2}{a}\sqrt{\frac{a^2-c^2}{c^2-b^2}}\,II(\vartheta_1, \frac{c^2k_1^2}{c^2-b^2}, k_1), \tag{A.3}$$

$$\sin^2\vartheta_1 = \frac{a^2(d^2-b^2)}{d^2(a^2-b^2)}, \tag{A.4}$$

$$\begin{aligned} H(c,d) &= c\ln\left(\frac{\sqrt{(c^2-b^2)(a^2-d^2)} + \sqrt{(a^2-c^2)(d^2-b^2)}}{\sqrt{(c^2-b^2)(a^2-d^2)} - \sqrt{(a^2-c^2)(d^2-b^2)}}\right) \\ &- \frac{2}{a}\sqrt{(d^2-b^2)(a^2-d^2)}\left\{F(\psi_2,k_1) + \frac{d^2}{a^2-d^2}II(\psi_2, \frac{a^2-b^2}{a^2-d^2}, k_1)\right\}, \end{aligned} \tag{A.5}$$

$$R_3 = \frac{2b^2}{a}\sqrt{\frac{a^2-d^2}{d^2-b^2}}\left\{F(\vartheta_1,k_1) - II(\vartheta_1, \frac{d^2-b^2}{d^2}, k_1)\right\} - d\ln\left(\frac{a^2-d^2}{a^2-b^2} + \frac{a^2(d^2-b^2)}{d^2(a^2-b^2)}\right)$$

$$+ \quad 2a\left(\frac{\pi}{2} - \psi_1 + \psi_2\right)\left\{E(\vartheta_1, k_1) - \frac{k_1^2 \sin\vartheta_1 \cos\vartheta_1}{\sqrt{1 - k_1^2 \sin^2\vartheta_1}}\right\} - 2R_2 F(\vartheta_1, k_1) - G(d, c), \tag{A.6}$$

$$R_4 = E(\vartheta_1, k_1) - \lambda_1^2 F(\vartheta_1, k_1) - \frac{k_1^2 \sin\vartheta_1 \cos\vartheta_1}{\sqrt{1 - k_1^2 \sin^2\vartheta_1}}, \tag{A.7}$$

$$\begin{aligned} R_5 &= -c \ln\left(\frac{(a^2 - c^2)(c^2 - b^2)}{c^2(a^2 - b^2)} + 1\right) + \frac{2}{a}\sqrt{\frac{c^2 - b^2}{a^2 - c^2}}\left\{a^2 F(\psi_2, k_1) - c^2 \Pi(\psi_2, \frac{a^2 - c^2}{a^2}, k_1)\right\} \\ &+ 2a\left(\frac{\pi}{2} - \psi_1 + \psi_2\right) E(\psi_2, k_1) - 2R_2 F(\psi_2, k_1) + H(c, d). \end{aligned} \tag{A.8}$$

## References


1. Gao H, Zhang TY, Tong P (1997) Local and global energy release rates for an electrically yielded crack in a piezoelectric ceramic. *J Mech Phy Solids* 45: 491–510.
2. Dugdale DS (1960) Yielding of steel sheets containing slits. *J Mech Phy Solids* 8: 100–104.
3. Ru CQ (1999) Effect of electrical polarization saturation on stress intensity factors in a piezoelectric ceramic. *Int J Solids Struct* 36: 869–883.
4. Ru CQ, Mao X (1999) Conducting cracks in a piezoelectric ceramic of limited electrical polarization. *J Mech Phy Solids* 47: 2125–2146.
5. Wang TC (2000) Analysis of strip electric saturation model of crack problem in piezoelectric materials. *Int J Solids Struct* 37: 6031–6049.
6. Li S (2003) On saturation-strip model of a permeable crack in a piezoelectric ceramic. *Acta Mech* 165: 47–71.
7. Jeong KM, Kim IO, Beom HG (2004) Effect of electric displacement saturation on the stress intensity factor for a crack in a piezoelectric ceramic. *Mech Res Comm* 31: 373–382.
8. Beom HG, Kim YH, Cho C, et al. (2006) A crack with an electric displacement saturation zone in an electrostrictive material. *Arch Appl Mech* 76: 19–31.
9. Fan CY, Zhao YF, Zhao MH, et al. (2012) Analytical solution of a semi-permeable crack in a 2*D* piezoelectric medium based on the PS model. *Mech Res Comm* 40: 34–40.
10. Bhargava RR, Jangid K (2014) A mathematical strip-saturation model for piezoelectric plate weakened by two collinear equal cracks. *Math Mech Solids* 19: 714–725.
11. Bhargava RR, Jangid K (2013) Strip-saturation model for piezoelectric plane weakened by two collinear cracks with coalesced interior zones. *Appl Math Modell* 37: 4093–4102.
12. Zhong HC, Lee KY (2014) Electroelastic fields induced by two collinear and energetically consistent cracks in a piezoelectric layer. *J Mech* 30: 361–372.

13. Sharma K, Bui TQ (2016) Numerical studies of an array of equidistant semi-permeable inclined cracks in 2-D piezoelectric strip using distributed dislocation method. *Int J Solids Struct* 80: 137–145.
14. Bui TQ (2014) Comparison of several BEM-based approaches in evaluating crack-tip field intensity factors in piezoelectric materials.*Int J Fracture* 189: 111–120.
15. Sharma K, Bui TQ (2013) Analysis of a subinterface crack in piezoelectric bimaterials with the extended finite element method. *Eng Fract Mech* 104: 114–139.
16. Muskhelishvili NI (1963) Some basic problems of the mathematical theory of elasticity, The Netherlands, Nordhoff.
17. Ou ZC, Wu X (2003) On the crack-tip stress singularity of interfacial cracks in transversely isotropic piezoelectric biomaterials. *Int J Solids Struct* 40: 7499–7511.


AIMS Press